

Time-Resolved ESR Study of Chromium(III) Complexes in the Ground State

Takashi Ikagawa, Takuhiro Otsuka, and Youkoh Kaizu*

Department of Chemistry, Tokyo Institute of Technology, O-okayama, Meguro-ku, Tokyo 152, Japan

Received: August 26, 1997; In Final Form: November 12, 1997

The time-resolved ESR (TR-ESR) signals of ground-state ($^4A_{2g}$) of Cr(III) ion were observed in ruby and of Cr(acac)₃ doped in Al(acac)₃ single crystals after irradiation with the second harmonic of a Nd:YAG laser at 77 K. At room temperature, TR-ESR signal was observed in ruby, but not in Cr(acac)₃. Both spectra at 77 K were of the emissive type; however, the intensity of the Cr(acac)₃ signal was very weak. The observed TR-ESR signal in ruby was changed from emissive polarity to an absorptive one at 700 μ s. The results of ruby and Cr(acac)₃ doped in Al(acac)₃ were explained by the initial emissive polarization and the recovery absorptive polarization from the excited state 2E . The spin polarization in the sublevels of the ground state was very long (about 500 μ s).

Introduction

In a previous paper, we briefly reported an observation of the photoinduced spin polarization in the ground state of Cr(III) in ruby at room temperature, by using TR-ESR technique.¹ The spin polarization on the 2E state was not observed, although the lifetime (3 ms at room temperature) of the excited state 2E_g is much longer than the time scale of the TR-ESR measurement (0.5 μ s). The TR-ESR signal was an emissive type initially and then changed to an absorptive type. Since the polarization shows the spin distribution in the ground state after laser excitation, the phase change of the signal indicates the reversal of the spin distribution among the ground-state sublevels. To clarify the origin and time dependence of spin polarization in the ground state of paramagnetic complexes, we measured TR-ESR spectra of Cr(acac)₃ doped in Al(acac)₃ and compared them with the results of ruby.

One hundred papers have been published on the chemistry of metal β -diketonates and their derivatives.^{2–7} Acetylacetone (2,4-pentandione) and other β -dicarbonyl compounds are very versatile and exhibit a great variety of coordination with metals in the usual bidentate behavior of monoanions.^{2,8} The crystal structure, electronic structure, and magnetic properties including ESR parameters have been studied by a number of researchers.^{5,9–13} The lifetime of the excited state of Cr(acac)₃ doped in Al(acac)₃ is affected by the environment of the complex and the temperature.⁵ Furthermore it has been reported that the quantum yield of the intersystem crossing from 4T_2 to 2E is very low, and the excited molecules in the 2E states are fewer than those of ruby.⁵ In the case of Cr(acac)₃, the internal conversion process from 4T_2 to 4A_2 is efficient; on the contrary, the process in ruby is disregarded because the quantum yield of the intersystem crossing is unity. In this paper, the TR-ESR technique was applied to the Cr(acac)₃ complex doped in Al(acac)₃ (Hacac = 2,4-pentandione) and ruby, and the results of TR-ESR were compared with each other. The spin polarization of Cr(acac)₃ was observed at 77 K but not at room temperature. We will report novel features of the spin polarization that occurred in the ground state 4A_2 of Cr(III) after visible light irradiation (532 nm) and discuss the mechanism and time-dependent spin polarization at the ground state of Cr(III) ions.

Experimental Section

Time-resolved direct detection CW-ESR (TR-ESR) measurements were carried out on a conventional X-band ESR spectrometer (JEOL, JES-RE1X) in the temperature range 77–300 K with a variable-temperature unit (ES-DVT2). To improve the time resolution (about 0.1 μ s per point) of the system, the field modulation was not used.

The samples were excited by a second harmonic of a Nd:YAG laser (Spectron, SL-401). The repetition rate was 20 or 10 Hz and laser power was about 15 mJ/pulse. Transient ESR signals were amplified with a wide-band amplifier (JEOL, ES-WBPA2) extended the dynamic range at 50 Hz to 7 MHz and then transferred to a transient memory (Kawasaki Electronics M-50E). Kinetic traces for each magnetic field position were stored and accumulated on a personal computer (NEC, PC-98FA). The response of the apparatus is checked by observing the TR-ESR signal of the triplet state of zinc tetraphenylporphyrin (ZnTPP).

The decay curves of the transient ESR signals were obtained by subtracting the kinetic decay at off-resonance conditions from those on resonance to get rid of electrical noise by the laser pulse. The kinetic decay was stored for about 5 ms. The baseline of the accumulation was used to average signals before laser irradiation. Thus we could obtain the signal's intensity versus time or magnetic field.

Cr(acac)₃ and Al(acac)₃, purchased from DOJINDO, were twice recrystallized from ethanol. Single crystals of Cr(acac)₃ in Al(acac)₃ were grown from ethanol by natural evaporation at room temperature. The Cr³⁺ concentration was about 1%. Single crystals were fixed in 3 mm o.d. quartz tube. The measurement at 77 K was accomplished in a liquid N₂ Dewar vessel. The crystal axes (*c* axis) of ruby and Cr(acac)₃ doped in Al(acac)₃ were determined by CW-ESR spectra. The measurement was accomplished by applying various static magnetic fields which made an angle θ with the *C*₃ axis of ruby. The angle μ is the angle of the *b* axis of Cr(acac)₃ with respect to the direction of the magnetic field. The wavelength of second harmonics ($\lambda = 532$ nm) was used for irradiation at the d–d states ($^4A_2 \rightarrow ^4T_2$) region of the Cr(III) ion. The beam direction is parallel to the magnetic axis.

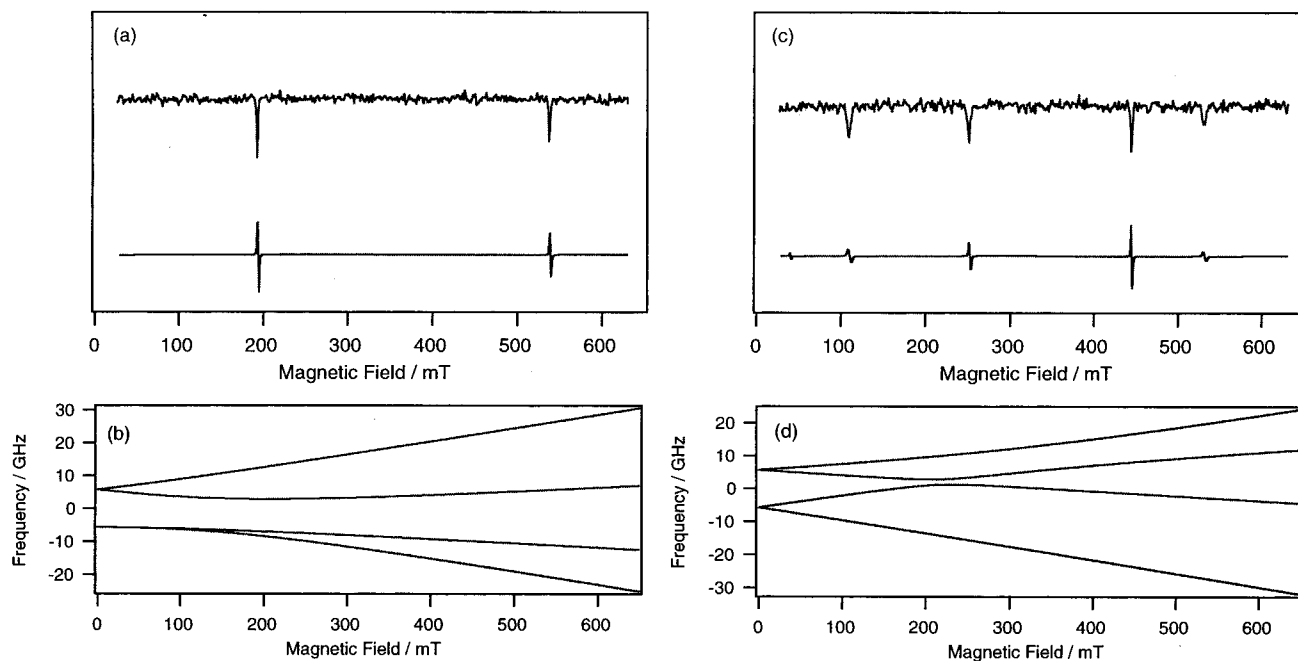


Figure 1. (a) TR-ESR (upper) and CW-ESR (lower) spectrum of ruby at room temperature ($\theta = 90^\circ$). (b) Schematic of the splitting of the basic level of the Cr(III) ion in ruby ($\theta = 90^\circ$). (c) TR-ESR (upper) and CW-ESR (lower) spectrum of ruby at room temperature ($\theta = 25^\circ$). (d) Schematic of the splitting of the basic level of the Cr(III) ion in ruby ($\theta = 90^\circ$).

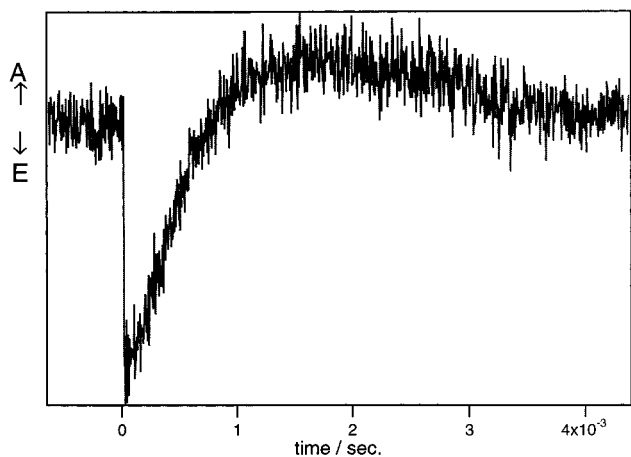


Figure 2. Decay curve of the TR-ESR signal of ruby at 193 mT.

Results

Figure 1a,c shows the TR-ESR (upper) and CW-ESR (lower) spectra of ruby at $\theta = 90^\circ$ and $\theta = 25^\circ$, respectively. TR-ESR spectra were taken 1 μ s after the laser pulse at room temperature. The CW-ESR spectra are shown with the first derivative of absorption. Both TR-ESR spectra show emissive type signals, and the resonance fields correspond to those of CW-ESR signals. These emissive signals corresponding with CW-ESR signals were observed at any angle. Therefore the signal obtained by TR-ESR is attributed to the spin polarization of the ground state after laser irradiation. There are no signals at the other fields and at other times except the signals corresponding to the ground state. In addition, the line shapes of the CW-ESR absorption signal and TR-ESR emissive signal are the same. These phenomena were observed at 77 K. The signal polarity was not changed by the laser light polarity (linear and circular).

Figure 2 shows the time dependence of the TR-ESR signal of ruby at low field (193 mT). The signal polarity was emissive type initially. The sign of the polarization changes at ≈ 700 μ s. The TR-ESR spectrum obtained after the polarity inversion gives precisely the same spectral shape as that just after the

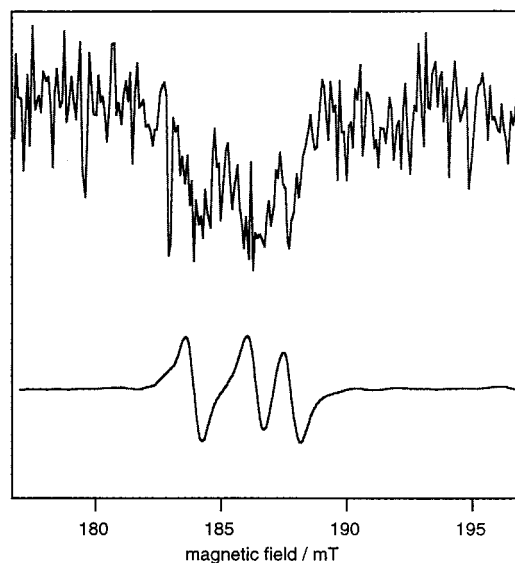


Figure 3. CW-ESR (lower) and TR-ESR (upper) spectra of Cr(acac)₃ in Al(acac)₃ at 77 K at $\mu = 90^\circ$.

laser excitation except for the sign of polarization: absorption spectra were obtained.

The CW-ESR and TR-ESR spectra of Cr(acac)₃ doped in Al(acac)₃ at 77 K are shown in Figure 3. The CW-ESR spectrum (Figure 3 (lower)) was shown in the first derivative of the absorption. The TR-ESR spectrum was obtained 0.5 μ s after the laser pulse. Figure 3 shows the spectra at $\mu = 90^\circ$. The spectra show some resonant fields at 77 K corresponding with a few sites of single crystal. The signals were only observed at CW-ESR resonant fields. The intensities of the emissive signals decreased as temperature rose to room temperature. At room temperature, there is no TR-ESR signal at any angle. The temperature dependence of the TR-ESR signal of Cr(acac)₃ is shown in Figure 4. The resonant fields of TR-ESR signals changed corresponding with those of CW-ESR signals. The lifetime of Cr(acac)₃ in the excited state 2E_g was 470 μ s at 77

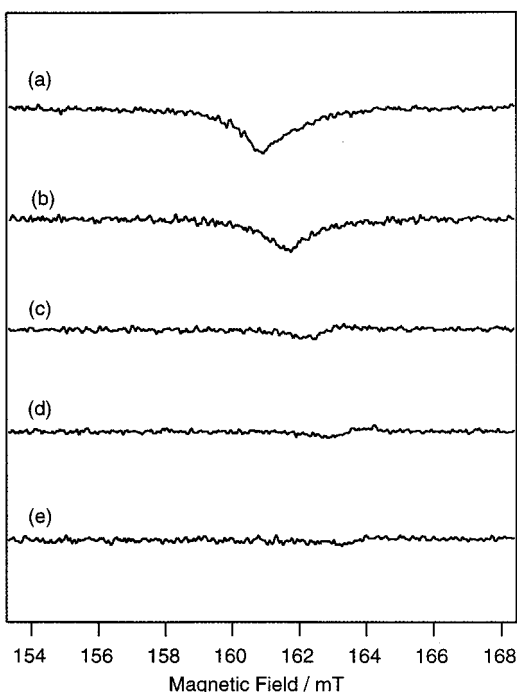


Figure 4. Temperature dependence of the TR-ESR signals at $\mu = 60^\circ$: (a) 123 K, (b) 173 K, (c) 223 K, (d) 273 K, (e) 300 K.

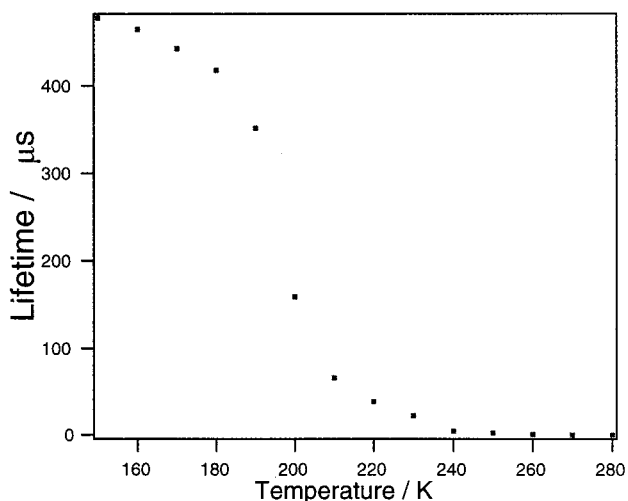


Figure 5. Temperature dependence of the lifetime of $\text{Cr}(\text{acac})_3$ in $\text{Al}(\text{acac})_3$.

K. Figure 5 shows the lifetime of emission from ${}^2\text{E}$ as a function of temperature. The lifetime is very short at 180–200 K and is submicrosecond at 250 K.

Discussion

Time-Resolved ESR Spectra of Ruby. The Cr(III) ion in ruby ($\text{Al}_2\text{O}_3:\text{Cr}^{3+}$) is in a site of trigonal symmetry C_3 . Parameters of ESR are reported as $D = -5.7235$ GHz, $g_1 = 1.984$, and $g_2 = 1.9867$.^{16,17} The Zeeman splitting of the ${}^4\text{A}_{2g}$ sublevels of Cr^{3+} in a magnetic field in ruby is shown in Figure 1 ((b) $\theta = 90^\circ$ and (d) $\theta = 25^\circ$). At $\theta = 90^\circ$, the transitions between various pairs of sublevels occur at two magnetic fields (about 193 and 534 mT at 9.42 GHz).

The electronic transition from the ground state ${}^4\text{A}_{2g}$ to the excited state ${}^4\text{T}_{2g}$ is caused by laser irradiation at 532 nm. The lifetime of the ${}^4\text{T}_{2g}$ state is considered to be very short. The intersystem crossing (ISC) arises from ${}^4\text{T}_{2g}$ to ${}^2\text{E}_g$ immediately, and the quantum yield is unity. As the decay time of the excited

state ${}^2\text{E}_g$ (3 ms at room temperature) is sufficiently long compared with the TR-ESR detection time scale, these signals reflect the spin population of the ground state and/or the excited state ${}^2\text{E}_g$. From the result that the TR-ESR signals correspond to the transition between ground-state sublevels, we can conclude that the signals are due to spin polarization of the ground state after excitation. Since the g -values of excited state ${}^2\text{E}_g$ have been reported as $g_{\parallel}(\bar{E}) = 2.445$ and $g_{\perp}(\bar{E}) < 0.06$,¹⁸ the observed signals do not correspond to the ${}^2\text{E}_g$ state. There were no signals at the other fields during the measurement time scale (0.1 μs to 5 ms) in this work. Despite the long lifetime at the excited state ${}^2\text{E}_g$, spin polarization was not observed. Since the spin relaxation is very fast among the ${}^2\text{E}_g$ sublevels, TR-ESR is silent in ${}^2\text{E}_g$. Y. Takagi et al. reported that the magnetization in ${}^2\text{E}_g$ was first observed at liquid He temperature.¹⁹

Furthermore a dependence upon laser wavelength was observed. The signal intensity for 355-nm laser irradiation was weaker than that of 532 nm when both pulse powers were same. The second-harmonic wavelength (532 nm) excites the d–d state at (${}^4\text{A}_{2g} \rightarrow {}^4\text{T}_{2g}$); however, that of third harmonic (355 nm) does not. Therefore, it is considered that the molecules of excited states produced by laser irradiation at 355 nm are less than those at 532 nm, so that the spin polarization becomes weak.

The emissive TR-ESR spectrum was observed at the ground state of the Cr(III) ion, as shown in Figure 1. The emissive spectrum implies that the population of the upper sublevel is higher than the lower among the ground-state spin sublevels compared with the Boltzmann distribution. There are two mechanisms for spin polarization in the ground state of Cr(III) ion. One is that the spin polarization occurs when the Cr(III) ion absorbs the light. Another is that the spin polarization is caused by the relaxation of the photoexcited state. The mechanism of spin polarization in this case is the former one for the following reasons: the quantum yield from ${}^4\text{T}_{2g}$ to ${}^2\text{E}_g$ is unity and the lifetime of ${}^2\text{E}_g$ is very long (3 ms at room temperature) in comparison with TR-ESR detection time: Figure 1 obtained at 1 μs after light irradiation. Thus the effect of the relaxation from the excited ${}^2\text{E}_g$ state to ground state ${}^4\text{A}_{2g}$ is negligible with the exception of the measurement at the later detection time. The spin polarization may be caused by the difference of absorption coefficients between ${}^4\text{A}_{2g}$ sublevels and ${}^4\text{T}_{2g}$ in the magnetic field; that is, the higher sublevels have smaller absorption coefficients than the lower sublevels.¹ At any angle, the emissive signals were observed for all resonant fields of the ground state.

Time-Resolved ESR Spectra of Tris(acetylacetonato)-chromium(III). The trisacetyl acetonatometal complexes crystallize in a monoclinic lattice with alternate stacking of right- and left-handed molecules. The symmetry axis of the molecules makes angles of 31° with the b axis; thereby there are two magnetically nonequivalent sites in the crystal.^{9,20} The ground state of ${}^4\text{A}_2$ and the excited states of ${}^2\text{E}$, ${}^4\text{T}_1$, and ${}^4\text{T}_2$ have been examined theoretically and experimentally.^{4,5,13} The d–d transition bands from ${}^4\text{A}_2$ to ${}^4\text{T}_2$ and ${}^4\text{T}_1$ are assigned to transitions at 17×10^3 and 24.5×10^3 cm^{-1} , respectively. The emission from ${}^2\text{E}$ to ${}^4\text{A}_2$ is observed at 12.7×10^3 cm^{-1} at a low temperature of 77 K and is not observed at room temperature.

The spin Hamiltonian of $\text{Cr}(\text{acac})_3$ is similar to that of ruby.¹⁷ The Cr(III) ions in $\text{Al}(\text{acac})_3$ are in a site of trigonal symmetry D_3 . These parameters are $g_x = 1.985$, $g_y = 1.990$, $g_z = 1.997$, $D = 0.597$ cm^{-1} , and $E = 0.0081$ cm^{-1} .⁵ The CW-ESR and TR-ESR spectra of $\text{Cr}(\text{acac})_3$ doped in $\text{Al}(\text{acac})_3$ at 77 K are

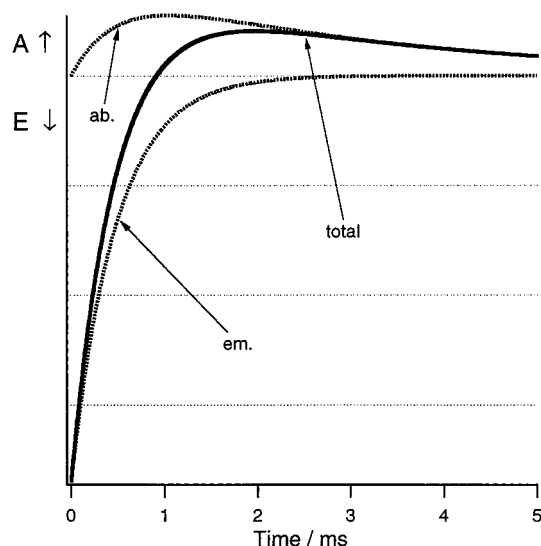


Figure 6. Simulation of TR-ESR signal decay: (a) absorption, (b) emission, (c) total.

shown in Figure 3. Since there are a few sites in the single crystal, the spectra show some resonant fields at 77 K. The TR-ESR signals corresponding with CW-ESR resonant fields were also observed; however, the intensities were very weak in comparison with that of ruby. The line shapes of the CW-ESR absorption signal and the TR-ESR emissive signal were the same. Therefore the signal obtained by TR-ESR was attributed to the spin polarization of the chromium complex ground state after laser irradiation. The TR-ESR signals were emissive type. The phase change of the TR-ESR signals was not observed.

The lifetime of $\text{Cr}(\text{acac})_3$ in the excited state ${}^2\text{E}$ was 470 μs at 77 K and varies from about 400 μs at 180 K to about 60 μs at 210 K (Figure 5). Although the lifetime is longer than the observation time of TR-ESR (0.5 μs) after light irradiation, the signal corresponding to resonant fields of ${}^2\text{E}$ could not be observed.

DeArmond and Forster reported that the emission quantum yield of $\text{Cr}(\text{acac})_3$ in EPA glass at 85 K was very low (0.03), and most of the initially excited molecules returned to the ground state directly from the ${}^4\text{T}_2$ state.²¹ The very weak TR-ESR signal of $\text{Cr}(\text{acac})_3$ doped in $\text{Al}(\text{acac})_3$ at 77 K suggests that the recovery of the ${}^4\text{T}_2$ state cancels out the TR-ESR signal just after light irradiation. The intensities of the emissive TR-ESR signals decreased as temperature rose (Figure 4 at $\mu = 60^\circ$). The TR-ESR signal was silent at room temperature. It is concluded that the decrease of the signal intensity indicates an increase in the direct recovery from ${}^4\text{T}_2$. In fact, the recovery from the ${}^4\text{T}_2$ state is dependent on temperature.²²

Polarity Change of the TR-ESR Signal. Figure 2 shows the time dependence of the TR-ESR signal of ruby at low field (193 mT). The sign of the polarization changes at $\approx 700 \mu\text{s}$. The absorptive TR-ESR spectrum gives precisely the same spectral shape as that just after the laser excitation except for the sign of polarization.

The time dependence of the ESR signal was not affected by the microwave (MW) power in this case. In general, on increasing the MW power (i) signal displays transient nutations due to the spin dynamics²³ and (ii) the initial spin polarization diminishes until it disappears. At resonance, the following relation holds for $M_y(t)$, which is proportional to the ESR signal,²⁴ at high MW power.

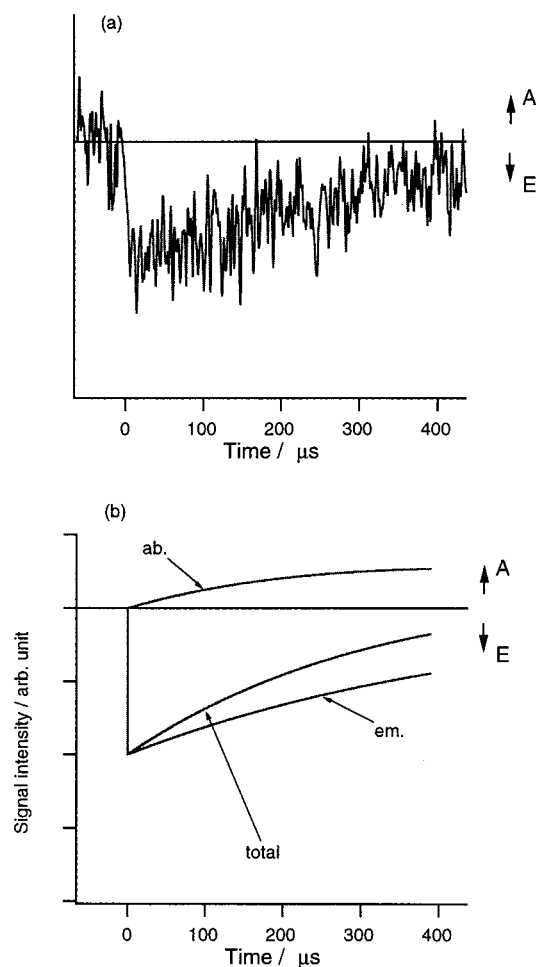


Figure 7. (a) Decay curve of $\text{Cr}(\text{acac})_3$ at 123 K. (b) Simulation ($a/b = 1.0$, $k = k' = 2090 \text{ s}^{-1}$).

$$M_y(t) = (\omega_1/b) \exp(at) \sin(bt) \quad (1)$$

where the parameters a and b are given by $a = -(T_1^{-1} + T_2^{-1})/2$, and $b = [\omega_1^2 - (T_2^{-1} - T_1^{-1})^2]^{1/2}$, respectively.

At moderate MW powers the signal decays in a single-exponential with a time constant T_1^{eff} given by $1/T_1^{\text{eff}} = 1/T_1 + \omega_1^2 T_2$. Equation 1 reduces to

$$M_y(t) = a' \exp(-t/T_{\text{eff}}) \quad (2)$$

The measured values of T_1^{eff} extrapolated to zero MW yield T_1 . In ruby, the decay curve could not be fit by eq 1 or 2. Thus, it must be considered that the effect of the recovery from the excited states is more than submilliseconds. On the basis of the polarity of the decay curve, we can assume that the absorptive polarity is caused by the recovery from ${}^2\text{E}_g$. The number of molecules relaxed from ${}^2\text{E}_g$ is proportional to $[a^*]_0 (1 - e^{-kt})$, where $[a^*]_0$ is the number of excited molecules just after the pulse irradiation and k is the rate constant of recovery from ${}^2\text{E}_g$, that is, the reciprocal of the phosphorescence lifetime. The recovered molecules have absorptive polarization and have the same spin relaxation rate of polarization as that of the initial polarization in the ground state. The polarization due to the recovered molecules at t is written as follows:

$$P_{\text{ab}} = \int_0^t \frac{d}{dt'} \{ [a^*]_0 (1 - e^{-kt'}) \} e^{-k'(t-t')} dt' \quad (3)$$

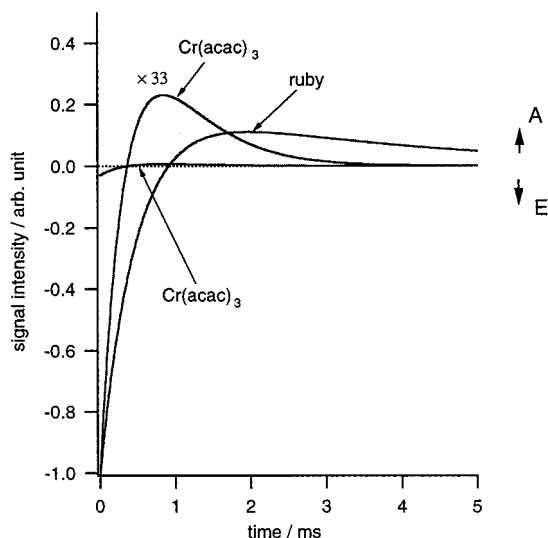


Figure 8. Simulation of the decay: $[b]_0(\text{ruby}):[b]_0(\text{Cr}(\text{acac})_3) = 1:0.03$.

where k' is the rate constant of spin relaxation. On the other hand, the emissive polarization produced by the excitation ($[b]_0$ at $t = 0$) is shown by eq 4.

$$P_{\text{em}} = -[b]_0 e^{-k't} \quad (4)$$

Therefore the whole polarization is given by

$$P_{\text{net}} = P_{\text{ab}} + P_{\text{em}} \quad (5)$$

$$= \begin{cases} ae^{-kt} - be^{-k't} & (k \neq k') \\ a'(t - b')e^{-kt} & (k = k') \end{cases} \quad (6)$$

where $a = [a^*]_0[k/(k' - k)]$, $b = [a^*]_0[k/(k' - k)] + [b]_0$, $a' = [a^*]_0k$, and $b' = [b]_0/[a^*]_0k$.

The decay curve shows a double exponential by using the function 6. The simulation is shown in Figure 6, where $k = 3.33 \times 10^2 \text{ s}^{-1}$, $k' = 2.09 \times 10^3 \text{ s}^{-1}$, and $[a^*]_0/[b]_0 = 1.33$. The k used is the reciprocal of the emission lifetime (3 ms). The initial polarization decay ($1/k' = 0.47 \text{ ms}$) is very long in comparison with the decay of an organic triplet (π, π^*) state. Furthermore the subsequent polarization is the same order as the emission decay. The polarity inversion can be explained by a recovery from 2E_g to ${}^4A_{2g}$ sublevels.

It is assumed that the spin polarization of $\text{Cr}(\text{acac})_3$ is given by the same equation as that of ruby. The decay curve can be simulated by using the same spin relaxation rate of the ground state as ruby ($k' = 2090 \text{ s}^{-1}$) and the reciprocal of the emission lifetime (k) of $\text{Cr}(\text{acac})_3$. Figure 7 shows the decay of the TR-ESR signal of $\text{Cr}(\text{acac})_3$ at 123 K and the simulation using the value of $[a^*]_0/[b]_0 = 1.0$ and $k = k' = 2090 \text{ s}^{-1}$. The simulation is in good agreement with the decay curve obtained.

Figure 8 shows the simulation at 123 K compared with that of ruby. The simulation also shows the change of polarity of $\text{Cr}(\text{acac})_3$ in the region 0.5–4 ms; however, the change of polarity of the TR-ESR signal cannot be observed in the $\text{Cr}(\text{acac})_3$ complex. In the $\text{Cr}(\text{acac})_3$ complex, intersystem crossing from 4T_2 to 2E may be less than 0.03. This means

that 97% of the excited molecules recover to the ground state immediately. The initial signal intensity is reduced by 1/33 compared with that of ruby. Thus it is likely that the very weak TR-ESR signal may prevent the measurement of a polarity change.

Conclusion

We observed that the long-lived spin polarization arises in the ground state of ruby at room temperature from irradiation of light. The spin polarization is caused by the difference in absorption coefficients for spin substates of ${}^4A_{2g}$ and ${}^4T_{2g}$. Absorptive TR-ESR spectra were obtained by the recovery from the 2E state.

On $\text{Cr}(\text{acac})$ doped in $\text{Al}(\text{acac})_3$, the emissive signals were obtained at 77 K, and the intensities were very weak. The decrease of the signal intensity means the increase of the direct recovery from 4T_2 . Moreover, it is considered that the recovery from 2E gives the absorptive polarization as well as ruby. The decay curve is interpreted by the initial polarization caused by light absorption followed by the recovery from the 2E state.

Acknowledgment. The authors are grateful to Professor Kin-ichi Obi, Tokyo Institute of Technology, for giving us a sample of ruby.

References and Notes

- (1) Ikagawa, T.; Otsuka, T.; Kaizu, Y. *Chem. Phys. Lett.* **1996**, 255, 248.
- (2) Fackler, J. P., Jr. *Prog. Inorg. Chem.* **1966**, 7, 361.
- (3) Jarrett, H. S. *J. Chem. Phys.* **1957**, 27, 1298.
- (4) Hanazaki, I.; Hanazaki, F.; Nagakura, S. *J. Chem. Phys.* **1969**, 50, 265.
- (5) (a) Barnum, D. W. *J. Inorg. Nucl. Chem.* **1961**, 21, 221. (b) Barnum, D. W. *J. Inorg. Nucl. Chem.* **1961**, 22, 183.
- (6) Kawaguchi, S. *Coord. Chem. Rev.* **1986**, 70, 51.
- (7) Joshi, K. C.; Pathak, V. N. *Coord. Chem. Rev.* **1977**, 22, 37.
- (8) Pike, R. M. *Coord. Chem. Rev.* **1967**, 2, 163.
- (9) Morosin, B. *Acta Crystallogr.* **1965**, 131, 19.
- (10) Forster, L. S.; DeArmond, K. *J. Chem. Phys.* **1955**, 23, 2193.
- (11) Piper, T. S.; Carlin, R. L. *J. Chem. Phys.* **1962**, 36, 3330.
- (12) Jarrett, H. S. *J. Chem. Phys.* **1957**, 27, 1298.
- (13) (a) Fields, R. A.; Haindl, E.; Winscom, C. J.; Khan, Z. H.; Plato, M.; Mobius, K. *J. Chem. Phys.* **1984**, 80, 3082. (b) Fields, R. A.; Winscom, C. J.; Haindl, E.; Plato, M.; Mobius, K. *Chem. Phys. Lett.* **1986**, 124, 121.
- (14) (a) Saunders, D. J.; Standley, K. J.; Wilson, P. G. *Br. J. Appl. Phys.* **1967**, 18, 1723. (b) Zaripov, M. M.; Shamonin, Iu. Ia. *Soviet Phys. JETP* **1956**, 3, 171. (c) Wenzel, R. F.; Kim, Y. W. *Phys. Rev.* **1965**, 140, 1592.
- (15) Singer, L. S. *J. Chem. Phys.* **1955**, 23, 379.
- (16) Pilbrow, J. R.; Sinclair, G. R.; Hutton, D. R.; Troup, G. J. *J. Magn. Reson.* **1983**, 52, 386.
- (17) Abragam, A.; Bleaney, B. *Electron Paramagnetic Resonance of Transition Ions*; Dover: New York, 1986; Chapter 7.
- (18) Geschwind, S.; Devlin, G. E.; Cohen, R. L.; Chinn, S. R. *Phys. Rev.* **1965**, 137, 1087.
- (19) Fukuda, Y.; Takagi, Y.; Hashi, T. *Phys. Lett.* **1974**, 48A, 183.
- (20) Astbury, W. T. *Proc. R. Soc.* **1926**, A112, 448.
- (21) DeArmond, K.; Forster, L. S. *Spectrochim. Acta* **1963**, 19, 1687.
- (22) Targos, W.; Forster, L. S. *J. Chem. Phys.* **1966**, 44, 4342.
- (23) (a) Hore, P. J.; McLauchlan, K. A. *J. Magn. Reson.* **1979**, 36, 129. (b) Hore, P. J.; McLauchlan, K. A. *Mol. Phys.* **1981**, 42, 533.
- (24) Atkins, P. W.; McLauchlan, K. A.; Percival, W. *Mol. Phys.* **1973**, 25, 281.